First-principles study of lateral atom manipulation assisted by structural relaxation of a scanning tip apex

Batnyam Enkhtaivan,[1] Yoshiaki Sugimoto,[2] and Atsushi Oshiyama[1]
[1]*Department of Applied Physics, The University of Tokyo, Hongo, Tokyo 113-8656, Japan*
[2]*Department of Advanced Materials Science, The University of Tokyo, Kashiwanoha 5-1-5, Kashiwa 277-8561, Japan*
(Received 3 June 2017; revised manuscript received 20 August 2017; published 6 October 2017)

We report first-principles density-functional calculations that elucidate mechanisms of atom manipulation with precise placement of the tip of a noncontact atomic force microscope (AFM). We focus on the vacancy-mediated lateral manipulation of the Si adatom on the Si(111)-(7 × 7) surface where intriguing adatom movement approaching (*approach move*) or following (*follow move*) the tip has been observed experimentally. We identify the diffusion pathways of the adatom from a stable position to another with and without the AFM tip and obtain the corresponding diffusion barriers. We find that a diffusion barrier as high as 1 eV without the AFM tip is reduced by a half eV with the assistance of the tip, indicating the increased feasibility of the adatom motion with the assistance of the AFM tip. More importantly, we find that the energy landscape of the adatom motion is modified drastically with the presence of the AFM tip: The most stable positions without the tip become metastable with the tip, whereas the metastable position becomes the most stable; the metastable position becomes unstable in some cases. We find that all these modifications of the energy landscapes depend on the atom-scale positioning of the AFM tip, inducing the spontaneous adatom move, i.e., the atom manipulation via the AFM tip. The obtained theoretical findings unveil the reason for the approach move and follow move. The underlying physics and chemistry of this atom manipulation are found to be the structural relaxation of the tip apex atom and the subsequent bond formation with the diffusing adatom.

DOI: 10.1103/PhysRevB.96.155417

I. INTRODUCTION

Noncontact (NC) atomic force microscopy (AFM) [1] has been successfully used in obtaining structural images of the surfaces of both conductive and nonconductive samples [2,3]. At present, the frequency modulation mode NC-AFM [4], in which the frequency shift of the oscillating cantilever caused by the tip-surface interaction from the resonant frequency is detected, is used to obtain atom-scale images of the surfaces. Beside surface imaging, utilizing such capability of the atomic resolution, it has also been used for the manipulation of a single atom on the surface [5–8].

The first AFM atom manipulation was performed by Oyabu *et al.* in 2003 [9], wherein they succeeded in pick-up and deposition of an adatom on the Si(111)-(7 × 7) surface at 78 K. Two years later, lateral manipulations of an adsorbate atom as well as an intrinsic adatom on the Ge(111)-c(2 × 8) surface were realized [10]. In the same year, Sugimoto *et al.* reported the first room-temperature atom manipulation by the AFM, wherein they interchanged the lateral positions of adjacent Sn and Ge adatoms on the Sn-covered Ge(111)-c(2 × 8) surface [11]. Following these pioneering works, various types of room-temperature atom manipulations have been realized. They include the vacancy-mediated lateral manipulation of an Si adatom on the Si(111)-(7 × 7) [12], the vertical interchange of the tip and the surface atoms on the Sn-covered Si(111)-($\sqrt{3} \times \sqrt{3}$)R30° [13], and the mechanical control (atom gating) of the inter-half-unit-cell diffusion of an adatom (Ag, Au, Si, Sn, or Pb) on the Si(111)-(7 × 7) surface [14].

Following the experimental advances, the microscopic mechanisms of the atom manipulations have been clarified by several theoretical studies. Atomistic calculations using a tight-binding method based on the density-functional theory (DFT) [15] have clarified that the formation of a dimer structure near the tip apex assists in the vertical interchange on the Sn-covered Si (111) surface [13]. Regarding the lateral interchange manipulation, we have proposed on the basis of the density-functional theory an adatom-exchange mechanism [16] in which the formation of multistable adatom dimers reduces the reaction barriers substantially. This resolves the discrepancy between the previous theoretical study [17,18] and the experiment [11]. We have also reported a detailed study of the atom gating manipulation clarifying the importance of the flexibility of the tip apex structure in the atom manipulation [19].

Notwithstanding those theoretical achievements, the observed phenomena in the atom manipulation are much more rich and complex and await theoretical clarification. An example which is experimentally investigated to great extent is the vacancy-mediated lateral manipulation of the intrinsic adatom on the Si(111)-(7 × 7) surface wherein bidirectional movement of a target adatom is induced by the proper placement of the AFM tip [12,20,21]: Upon line scanning of the AFM tip, a target adatom moves following the AFM tip (*follow move*) and/or approaching the AFM tip (*approach move*). Details of the experimental observation are as follows. There are six Si adatoms in a half unit cell (HUC) of the Si(111)-(7 × 7) dimer-adatom-stacking-fault structure [22] [Fig. 1(a)]. Sugimoto *et al.* have prepared an adatom vacancy in a HUC and performed the line scanning of the AFM tip from the initial corner adatom site [Co site in Fig. 1(b)] to the final other corner adatom site via the center adatom site [Ce site in Fig. 1(b)] [12]. At the beginning the adatom, vacancy exists at the Ce site. In the lateral manipulation with this line scanning, the adatom at the Co site moves to the Ce site, leaving the vacancy at the Co site. Careful analyses [12,20,21] of the

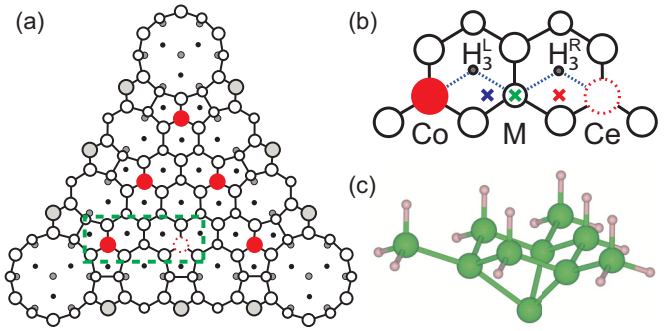

FIG. 1. (a) Schematic top view of the half unit cell (HUC) of Si(111)-(7 × 7). The circles depict the atomic sites with their sizes reflecting the closeness to the surface top. Six adatom sites in the HUC are shown by red circles including a single vacant site (dotted circle). (b) The close-up view of the region surrounded by the green line in (a). The blue dashed lines illustrate the adatom diffusion pathway. The corner adatom site (Co), the center adatom site (Ce), and other metastable sites (M and H_3) for an adatom are shown. To distinguish between the two H_3 sites on the diffusion pathway, we add superscripts "L" and "R" to the left and right H_3 sites, respectively. The green, blue, and red x marks show the lateral tip positions considered, and are named as position M, position L, and position R, respectively. (c) The model of the Si tip considered in the calculation. The green (large) and beige (small) spheres depict Si and H atoms, respectively.

line profiles reveal the existence of the follow move and the approach move of the adatom. When the AFM tip is scanned from the Co site and placed near the M site, the adatom at the Co site moves to the M site and follows the AFM tip to the Ce site (follow move). In the subsequent scanning, when the AFM tip comes to the M site, the adatom at the Ce site moves to the M site (approach move) and then moves back to the Ce site with the AFM tip (follow move). In another scanning from the vacant Ce site to the adatom Co site, when the AFM tip comes to the M site, the adatom welcomes the tip at the M site (approach move) and then moves back to the Co site following the tip scanning (follow move).

Frequency of the AFM cantilever is an order of 100 kHz whereas the typical time scale of the adatom motion is 1 ps or 1 ns at the longest. Hence the lateral atom manipulation by the NC-AFM is regarded as modulation of atomic diffusion by the AFM tip. Theoretical calculations in the past indeed have clarified that the energy barrier of the atomic diffusion on the surface is lowered due to the covalent interaction between the tip apex atom and the adatom [12,16,19,21]. The follow move described above may be understandable along this line. However, the approach move is mysterious since the tip-adatom distance is expected to be large enough (nominally 4 Å) to prevent the tip apex and the adatom from the covalent interaction. Further, in spite of the metastability of the H_3 site found in the previous theoretical works [12,21], the adatom is never observed at the H_3 site during the lateral manipulation. There are certainly unclarified problems which await the theoretical approach.

In this paper, we consider the microscopic mechanism for the follow move and the approach move during the lateral manipulation with the NC-AFM tip. Our DFT calculations performed for the adatom diffusion on the Si(111)-(7 × 7) surface clarify the modulation of the diffusion barrier due to the presence of the NC-AFM tip and explain all the observations during the lateral manipulation. We find that the essential reason for the approach move is the structural relaxation of the tip apex atom that allows the covalent interaction even at the large nominal tip-adatom distance.

The paper is organized as follows. The calculational methods and the pertinent conditions for the calculations are explained in Sec. II. The lateral diffusion of the Is adatom without the AFM tip is described in Sec. III A. In Secs. III B 1, III B 2, and III B 3, the modifications of the adatom diffusion by the Si tip at three different positions are described. Finally, we summarize our findings in Sec. IV.

II. CALCULATIONS

Calculations have been performed within the framework of the density functional theory [23,24]. The generalized gradient approximation [25,26] is used for the calculation of the exchange-correlation energy. We have adopted the plane-wave/pseudopotential approach using the Vienna *ab initio* simulation package [27,28]. Projector augmented wave potentials [29,30] are adopted to describe the electron-ion interaction. The cutoff energy of the plane-wave basis is 250 eV.

The Si(111)-(7 × 7) surface is simulated by a repeating slab model in which an atomic slab consists of six atomic layers plus an adatom layer and is separated from its adjacent images by the vacuum region. The atomic distances between the different slabs are more than 6 Å, which is found to be large enough to neglect the interaction between the slab and its images [16]. In the calculations without the AFM tip, the slabs are separated with more than 8-Å distance. The atoms at the bottom-most layer of each slab are terminated with H atoms to saturate the artificial dangling bonds. In the lateral directions, the Si(111)-(7 × 7) surface is simulated by the single surface unit cell of the dimer-adatom-stacking-fault model [22]. Only the Γ point is sampled for the Brillouin-zone integration since the supercell cells are large. The structural relaxation is performed using the conjugate-gradient algorithm utilizing the Hellmann-Feynman forces. All the atoms except for the H atoms and the Si atoms bonded with them are relaxed until the forces acting on the atoms are smaller than 0.1 eV/Å [31].

To identify the reaction pathways of the adatom diffusion and the corresponding energy barriers, we adopt the climbing-image nudged elastic band (CINEB) method [32]. This method identifies a saddle-point geometry and its energy partly assuring the continuity of the reaction pathway compared with the hyperplane constraint method [33] by introducing fictitious elastic forces during the constraint energy minimization. For each probable diffusion pathway, we have first explored all the stable and metastable configurations in the vicinity of the pathway by the geometry optimization. Then given the two adjacent (meta)stable configurations, we have chosen three image configurations and performed a CINEB search to determine the pathway. Repeating this treatment for the pathways between all the (meta)stable configurations, we have obtained the whole diffusion pathway which is the most probable. The search for the (meta)stable configurations have been carried out in the case without the AFM tip. With the

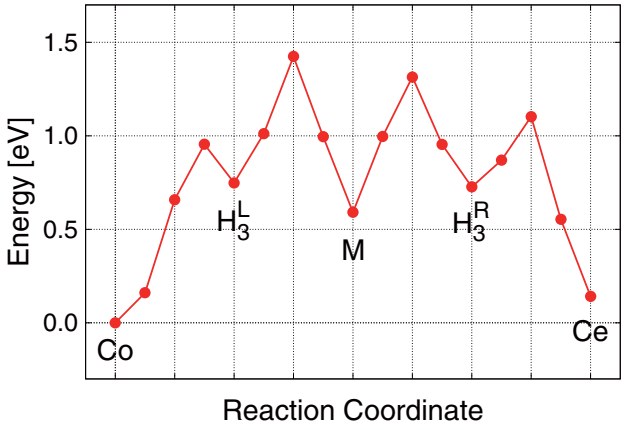

FIG. 2. The energy profile of the diffusion of an Si atom between the corner adatom (Co) site and the center adatom (Ce) site, as illustrated in Fig. 1(b). The abscissa is the reaction coordinate taken along the reaction pathway. The ordinate is the energy of the system measured from that of the system in which the Si atom is located at the Co site.

presence of the AFM tip, the search for the (meta)stable configurations is done in the vicinity of the (meta)stable configurations without the AFM tip.

The AFM Si tip is simulated by an atomistic model consisting of 10 Si atoms and 15 H atoms as shown in Fig. 1(c). This model is used in a number of previous works in simulating the Si tip of the AFM [12,16,19,21,34–38]. In our calculations, we have done structural relaxation of the tip along with the surface atomic configurations. The H atoms and the Si atoms bonding with the H atoms in the Si tip, however, are fixed during the geometry optimization.

III. RESULTS

A. Lateral diffusion of the Si adatom without the AFM tip

We consider the diffusion of an adatom located at the Co site to the vacant site Ce and vice versa corresponding to the experimental situation.

Prior to the calculation of the energy profile, we have confirmed that the H_3 and the M sites are (meta)stable as reported in the previous calculations [12,21]. At these sites, the adatom bonds with the three Si atoms of the lower layer, which makes those sites (meta)stable. Then, we find that the adatom diffuses by passing through them, i.e., the Co-H_3^L-M-H_3^R-Ce pathway. This pathway is the same as the diffusion pathway in the previous report [12].

The calculated energy profile of the adatom diffusion between the Co and Ce sites without the presence of the AFM tip is shown in Fig. 2. The energy profile is almost symmetric with respect to the M position, reflecting the structural similarity between the Co-M and M-Ce regions. The total energy of the Co site is slightly lower (by 0.14 eV) than that of the Ce site, indicating that the binding energy of the adatom at the Ce site is larger than that at the Co site. This is in perfect agreement with the previous experiment [39]. Between two of the stable or metastable sites, there is an energy barrier which the adatom is required to overcome. We have found four distinct energy barriers in the diffusion from the Co to the Ce and vice versa, indicative of the multistep diffusion process. In the diffusion from the Co to the Ce, for instance, the barriers are 0.95 eV (Co $\rightarrow$ H_3^L), 0.67 eV (H_3^L $\rightarrow$ M), 0.72 eV (M $\rightarrow$ H_3^R), and 0.37 eV (H_3^R $\rightarrow$ Ce). The rate-determining process is the Co $\rightarrow$ H_3^L diffusion with the corresponding barrier of 0.95 eV. Similarly, in the reverse Ce $\rightarrow$ Co diffusion, the rate-determining process is the Ce $\rightarrow$ H_3^R diffusion with the energy barrier of 0.96 eV. In both directions, the diffusion barriers are as high as 1 eV, indicating that the adatom diffusion is infrequent on the Si(111)-(7 $\times$ 7) at room temperature.

By comparing the obtained energy barriers with the previously reported results (Table 1 in Ref. [12]) [40], we find that the the barriers previously reported are higher than the present values. We provisionally ascribe this discrepancy to the difference in the computational method, i.e., the present DFT scheme and the tight-binding scheme based on the DFT in Ref. [12].

B. Lateral diffusion of the Si adatom with the AFM tip

The modifications of the adatom diffusion by the AFM tip are studied by placing the tip at three different positions, i.e., *position M*, *position L*, and *position R* as shown in Fig. 1(b). We choose these tip positions since at these tip positions the adatom movement is observed in the experiment [12]. For each of the lateral tip positions, we calculate the energy profile of the adatom diffusion with three different tip-surface distances, i.e., 3.0, 4.0, and 4.5 Å, to clarify atom-scale variation of the tip-surface interaction. Here, the tip-surface distance denotes the nominal distance between the tip apex atom and the surface adatom before the structural relaxation.

1. The adatom diffusion with the tip at position M

The energy profiles of the adatom diffusion when the tip is placed at position M is shown in Fig. 3.

When the tip-surface distance is 4.5 Å, the calculated energy profile shows significant energy decrease around the M site whereas it is almost unchanged near the Co, Ce, H_3^L, and H_3^L sites. As a result, the energy barriers of the Co $\rightarrow$ H_3^L and the Ce $\rightarrow$ H_3^R diffusion pathways are not reduced. This is due to the weak interaction between the tip apex atom and the adatom near the Co, Ce, H_3^L, and H_3^L sites: The distances between the tip apex atom and the adatom adsorbed at the Co site and the H_3^L site after the structural optimization are 5.9 and 5.1 Å, respectively. On the other hand, the total energy near the M site is significantly reduced. At the M site the reduction is 0.48 eV. The reduction around the M site leads to the reduction of the diffusion barrier from either the H_3^L site or the H_3^R site to the M site. The energy barrier for the H_3^L $\rightarrow$ M decreases to be 0.14 eV. Also the barrier for the H_3^R $\rightarrow$ M decreases to be 0.19 eV from the value 0.59 eV without the tip. The obtained energy reduction is due to the significant interaction between the tip and the adatom. In the M site configuration, the distance between the tip apex atom and the adatom is 3.4 Å after structural optimization.

The energy profile is modified more significantly with the further approach of the tip to the tip-surface nominal distance of 4.0 Å (black rectangles in Fig. 3). Due to the strong

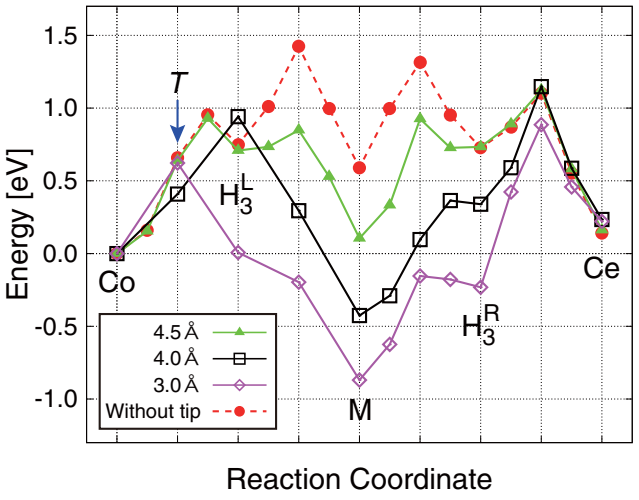

FIG. 3. The energy profiles of the diffusion of an Si atom between the corner adatom (Co) site and the center adatom (Ce) site with the AFM tip being placed at the M site. The axes and the labels are the same as those of Fig. 2. The green (triangle), black (rectangle), and magenta (diamond) lines are energy profiles of the adatom diffusion when the tip-surface nominal distances are 4.5, 4.0, and 3.0 Å, respectively. The red (circle) dashed line is the energy profile of the adatom diffusion without the presence of the AFM tip.

interaction with the tip, the total energy of the system in which the adatom is located at the M site is further reduced by 0.53 eV compared with the case of the tip-surface nominal distance of 4.5 Å, making this site most stable. The distance between the tip apex atom and the surface adatom becomes 2.8 Å after the structural optimization. This distance is close to the bond length in Si crystal (2.35 Å). At this tip-surface distance, the structure where the adatom is located at the H_3^L site is no longer metastable, leading to the spontaneous movement of the adatom from the H_3^L to the M site. Consequently, the diffusion of the adatom from the Co site to M site is a one-step reaction. Similarly, the H_3^R site is almost unstable in a sense that the energy barrier for escaping from this site is overcome by the thermal fluctuation at room temperature. This theoretical finding perfectly explains the experimental fact [12] that the adatom is never observed at the H_3 site during the lateral manipulation.

To clarify the nature of the interaction between the tip and the surface, we have calculated the electron density difference between the combined system of the tip and the surface and a system in which the tip and the surface are isolated. In Fig. 4(a), such electron density difference is shown for the tip-surface nominal distance of 4.0 Å. The electron density decreases around the tip apex atom and the surface adatom and it increases in the region between them, indicating the formation of the covalent bond. This bond formation is accompanied with the structural modification: The tip apex atom and the surface adatom move toward each other by 0.67 and 0.55 Å, respectively, from their original positions in the isolated configuration.

The M site is further stabilized by 0.44 eV with the approach of the tip to the nominal distance of 3.0 Å from the surface (the magenta diamonds in Fig. 3). Interestingly, at this

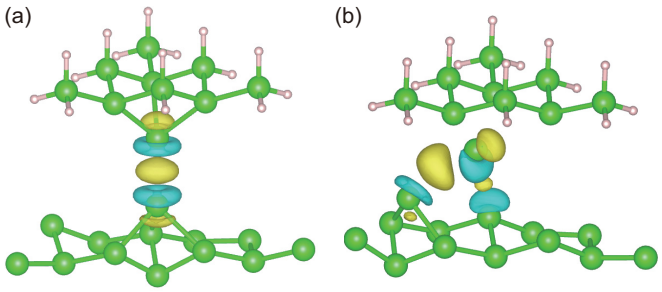

FIG. 4. Electron density with the presence of the AFM tip at the M site. (a) The electron density when the adatom is located at the M site with the tip-surface nominal distance of 4.0 Å. The density difference between the combined tip-surface system and the isolated tip plus the isolated surface system is shown. (b) The electron density difference at the *T* configuration shown in Fig. 3 with the tip-surface nominal distance of 3.0 Å. The green and the beige circles depict Si and H atoms. The yellow and blue regions show the isosurfaces (30% of the maximum value) of the region where the electron density is increased and decreased, respectively.

tip-surface nominal distance, the diffusion barriers from the Co and Ce sites to the M site are reduced to be 0.62 and 0.66 eV, respectively. We have found that the barrier reduction occurs due to the relaxation of the tip apex configuration. Figure 5 shows the structural relaxation of the tip apex atom during the adatom diffusion. The structural analysis shows that the tip apex atom shifts from its unrelaxed position by as much as 1.0 Å in the lateral plane toward the diffusing atom. The electron density clearly shows the origin of this substantial shift of the tip apex atom. Figure 4(b) shows calculated electron density difference for the *T* configuration depicted in Fig. 3. Even though there are several regions where the electron density is increased, the largest increase occurs in

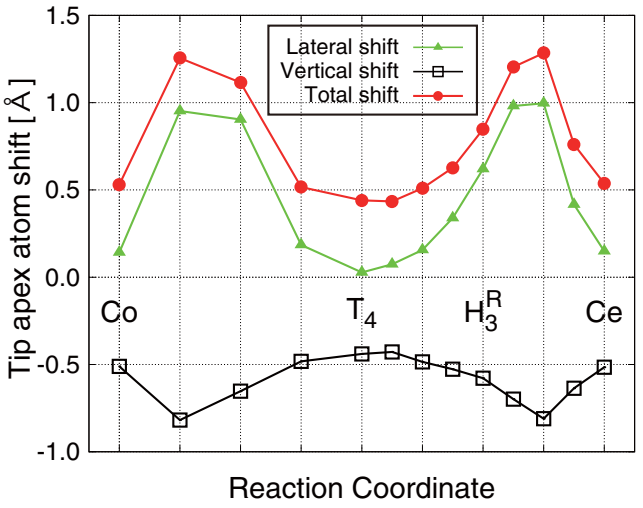

FIG. 5. Structural relaxation of the tip apex atom with the tip-surface nominal distance of 3.0 Å as a function of the adatom position. The red circle is the shift of the tip apex atom from its original position without the surface. The green triangle and black square show the shift of the tip apex atom in the lateral plane and the vertical direction, respectively.

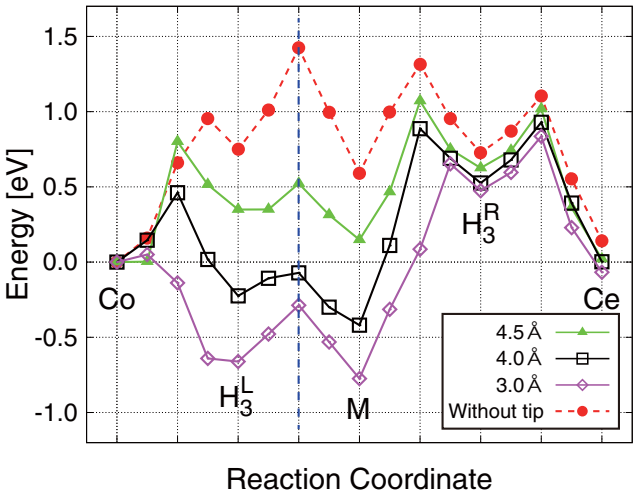

FIG. 6. The energy profiles of the diffusion of an Si atom between the corner adatom (Co) site and the center adatom (Ce) site with the AFM tip being placed at the position L. The axes and the labels are the same as those of Fig. 2. The green (triangle), black (rectangle), and magenta (diamond) lines are energy profiles of the adatom diffusion when the tip-surface nominal distances are 4.5, 4.0, and 3.0 Å, respectively. The red (circle) dashed line is the energy profile of the adatom diffusion without the presence of the AFM tip. The blue dashed vertical line is the guide for the eye to show the (approximate) position of the tip.

the middle of the tip apex atom and the diffusing adatom, indicating substantial interaction between them. When the tip atoms are not allowed to relax, the energy barriers of the Co → M and Ce → M diffusion processes are found to be not lowered. This clearly indicates the importance of the shift of the tip apex atom in the atom manipulation. The enhanced diffusion from the Co site to the M site and also from the Ce site to the M site obtained above with the presence of the AFM-tip near the M site perfectly explains the observed mysterious approach move in the experiment (Figs. 2(b)-B and 2(b)-D in Ref. [12]).

2. *The adatom diffusion with the tip at position M*

The calculated energy profiles of the adatom diffusion when the tip is placed at position L are shown in Fig. 6. Position L is near the center of the H_3^L and the M sites. Hence, the energy profile of the adatom diffusion becomes significantly asymmetric. When the tip-surface distance is 4.5 Å, the diffusion barrier of Co → H_3^L is reduced from its tipless value to be 0.80 eV. Interestingly, the total energy of the second image structure (nudged elastic band image structure shown by the green triangle next to the Co in Fig. 6) of the the Co → H_3^L diffusion is almost the same as that of the initial state (adatom located at the Co site). This is due to the compensation of the energy loss caused by the adatom dislodged from the Co site by the energy gain from the interaction between the adatom and the tip apex atom.

The adatom at the H_3^L site is significantly more stabilized than the adatom at the H_3^R site. This is obviously due to the difference in the strength of the interaction between the adatom and the tip apex atom. When the adatom is located at the H_3^R site, the distance between these two atoms is 5.6 Å even after the structural optimization, while it is 3.6 Å when the adatom is located at the H_3^L site. The total energy of the adatom located at the M site is also lowered. The distance between the tip apex atom and the surface adatom located at the M site is 3.5 Å. Consequently, the energy barrier for H_3^L → M diffusion is reduced to be 0.17 eV, about a quarter of the tipless value. Unlike the diffusion from the Co site to the M site, the energy barrier of the diffusion from the M site to the Ce site is not reduced. It is rather increased to be 0.92 eV.

Then, as the tip further approaches the surface to the 4.0-Å nominal distance, the diffusion barrier of Co → H_3^L is further reduced and becomes 0.46 eV. The total energies of the atomic configurations in which the adatom is adsorbed at either the H_3^L or the M site are significantly lowered. Consequently, the M site becomes the most stable site for the adatom. The energy barrier of H_3^L → M is slightly reduced from 0.17 to 0.15 eV. The distances between the tip apex atom and the adatom located at the H_3^L and M sites are 2.8 Å. The reduction of the energy barrier of Co → M diffusion and the stabilization of the adatom location at the M site show that the diffusion from the Co site to the M site is enhanced by the presence of the tip. The energy barrier of the reverse diffusion (H_3^L → Co) is increased to be 0.69 eV from the value 0.45 eV for the tip-surface nominal distance of 4.5 Å, showing that the reverse diffusion is hindered by the presence of the tip. In contrast with the Co → M diffusion, the energy barrier of M → H_3^R diffusion increases to 1.31 eV. Such a high barrier shows that the adatom does not diffuse from the M site to the Co site, and stays at the M site.

Similarly, when the tip-surface nominal distance becomes 3.0 Å, the total energies of the H_3^L and M sites are lowered by 0.44 and 0.36 eV compared to the total energy of the Co site. Accompanying this stabilization of the intermediate states, the energy barrier of Co → H_3^L is reduced and becomes 0.05 eV. Unlike the diffusion from the Co site to the M site, the energy barrier of the diffusion from the M site to the H_3^R site increases to be 1.42 eV. The calculated result for the tip at position L perfectly explains the experimentally observed [12] follow move wherein the adatom moves from the Co site to the M site following the AFM tip placed around the M site (Fig. 2(b)-C in Ref. [12]).

3. *The adatom diffusion with the tip at position M*

Position R is the center of the the M and the Ce sites. The energy profiles of the adatom diffusion between the Co and Ce sites when the tip is placed at position R are shown in Fig. 7. Let us first explain the energy profile of the adatom diffusion when the tip-surface distance is 4.5 Å. The energy barriers of the Ce → H_3^R and the M → H_3^R diffusions are significantly reduced from their tipless values to be 0.45 and 0.21 eV, respectively. However, the energy barriers of the H_3^R → Ce and the H_3^R → M diffusions do not change much. This difference in the barrier reduction is due to the difference in the stabilization of the adatom adsorption among the M, H_3^R, and Ce sites. The energy of the system in which the adatom is at the H_3^R site decreases much more than the energy of the system in which the adatom is at the Ce and M sites. The distance between the tip apex atom and the adatom located at the H_3^R site is 3.5 Å after the

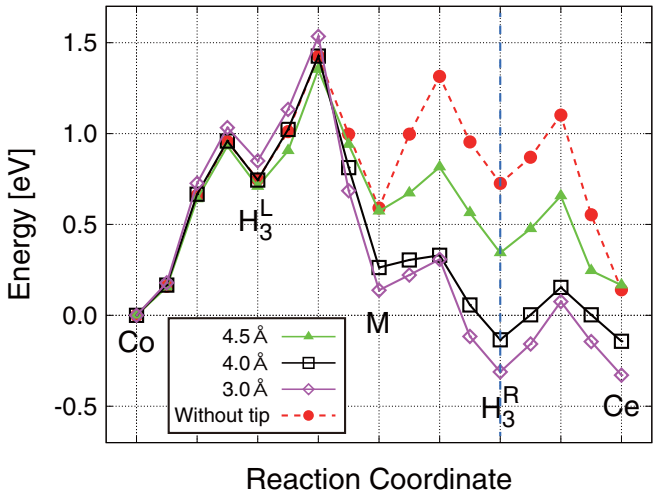

FIG. 7. The energy profiles of the adatom diffusion between the Ce and M sites with the AFM tip being placed at the position M. The green (triangle), black (rectangle), and magenta (diamond) lines are energy profiles of the adatom diffusion when the tip-surface nominal distances are 4.5, 4.0, and 3.0 Å, respectively. The red (circle) dashed line is the energy profile of the adatom diffusion without the presence of the AFM tip. The blue dashed vertical line is the guide for the eye to show the (approximate) position of the tip.

geometry optimization, while the distances at the Ce and the M sites are 4.8 and 4.2 Å, respectively.

When the tip approaches the surface at the nominal distance of 4.0 Å, the energy barriers of the Ce $\rightarrow$ H_3^R and the M $\rightarrow$ H_3^R diffusions are further reduced and become 0.28 eV. On the other hand, the energy barriers of the H_3^R $\rightarrow$ Ce and the H_3^R $\rightarrow$ M diffusions remain almost unchanged since the energies of the H_3^R state and the two transition states are lowered by almost the same amount.

The diffusion barriers of the Ce $\rightarrow$ H_3^R and the H_3^R $\rightarrow$ M diffusions slightly increase with the approach of the tip with the the tip-surface nominal distance of 3.0 Å. At the transition state, the distance between the tip apex atom and the diffusing adatom is reduced by 0.33 Å (from 2.69 to 2.36 Å) accompanying the approach of the tip. On the other hand, the distances between the tip apex atom and the adatom located at the Ce and H_3^R sites are reduced by 0.53 and 0.38 Å, respectively. Therefore, the energy gain at the transition state is smaller than the energy gains at the Ce and the H_3^R sites. Also, even with the approach of the tip to the surface, the energy of the M site relative to the Ce site is almost unchanged. This is not because the tip is not interacting with the adatom at these sites, but because the energy gain due to the interaction is similar for these adsorption sites. The distances between the tip apex atom and the adatom in these sites are 2.8 Å (M site) and 3.0 Å (Ce site) after the geometry optimization.

We have found that the diffusion from the M to the Ce site is enhanced with the presence of the AFM tip at the center of them. The rate-determining barrier is reduced from 0.72 eV with the absence of the tip to 0.31 eV (the nominal tip-surface distance of 4.5 Å), 0.28 eV (the nominal distance of 4.0 Å), or 0.39 eV (the nominal distance of 3.0 Å) with the presence of the tip. This theoretical finding perfectly explains the follow move experimentally observed, i.e., follow moves from M_L to Ce sites (Figs. 2(b)-C and 2(b)-D in Ref. [12]). The observed follow move from the M_R to the Co site (Fig. 2(b)-B in Ref. [12]) is also explained by the obtained energy profile since the geometrical arrangement for the adatom at the Co site is similar to that at the Ce site.

IV. SUMMARY

We have elucidated the mechanisms of atom manipulation at room temperature on the Si(111)-(7 $\times$ 7) surface with the probe of the noncontact atomic force microscope on the basis of first-principles density-functional calculations. We have focused on the vacancy-mediated lateral manipulation of the Si adatom in which a mysterious approach move and follow move of the adatom with the assistance of the atomic probe have been observed experimentally. Recognizing that the manipulation with the NC-AFM is essentially the modification of the adatom motion with the presence of the AFM tip, we have identified the diffusion pathways of the adatom from a stable position to another with and without the AFM tip and obtained the corresponding diffusion barriers. Without the AFM tip, we have found that the adatom diffusion takes place via the multistep process in which the adatom moves through several metastable configurations. The energy barrier of the rate-determining process in the diffusion between the two stable positions is found to be as high as 1 eV. We have found that this barrier is formidable to overcome at room temperature and is reduced by the presence of the AFM tip by a half eV depending on the position of the AFM tip, indicating the increased feasibility of the adatom motion with the assistance of the AFM tip. More importantly, we have found that the energy landscape of the adatom motion is modified drastically with the presence of the AFM tip: The most stable positions (Co and Ce sites in this paper) without the tip become metastable with the tip, whereas the metastable position (M in this paper) becomes the most stable; further, the metastable position (H_3 in this paper) becomes unstable in some cases. All these modifications of the energy landscapes depend on the atom-scale position of the AFM tip. Consequently, the adatom moves spontaneously following (follow move) or approaching (approach move) the AFM tip. This unveils the reason for the mysterious move of the adatom by the AFM tip experimentally observed and also opens a possibility of more sophisticated atom manipulation with the precise positioning of the AFM tip. The underlying physics and chemistry of this modification of the energy landscape are the flexible structural relaxation of the tip apex atom and the subsequent bond formation with the diffusing adatom. We have found that the tip apex atom dislodged from its unrelaxed position by as much as 1.3 Å during the adatom diffusion so as to form a covalent bond with the diffusing atom. The bond formation is unequivocally evidenced by our calculated electron density.

ACKNOWLEDGMENTS

This paper was supported by the Ministry of Education, Culture, Sports, Science, and Technology as a social and

scientific priority issue (Creation of new functional devices and high-performance materials to support next-generation industries) to be tackled by using a post-K computer. Computations were performed mainly at the Supercomputer Center at the Institute for Solid State Physics, The University of Tokyo, The Research Center for Computational Science, National Institutes of Natural Sciences, and the Center for Computational Sciences, University of Tsukuba.

[1] G. Binnig, C. F. Quate, and C. Gerber, Phys. Rev. Lett. **56**, 930 (1986).
[2] F. J. Giessibl, Rev. Mod. Phys. **75**, 949 (2003).
[3] *Noncontact Atomic Force Microscopy*, edited by S. Morita, R. Wiesendanger, and E. Meyer (Springer-Verlag, Berlin, 2002).
[4] T. R. Albrecht, P. Grütter, D. Horne, and D. Rugar, J. Appl. Phys. **69**, 668 (1991).
[5] O. Custance, R. Perez, and S. Morita, Nat. Nano **4**, 803 (2009).
[6] M. Ternes, C. P. Lutz, C. F. Hirjibehedin, F. J. Giessibl, and A. J. Heinrich, Science **319**, 1066 (2008).
[7] M. Emmrich, M. Schneiderbauer, F. Huber, A. J. Weymouth, N. Okabayashi, and F. J. Giessibl, Phys. Rev. Lett. **114**, 146101 (2015).
[8] S. Kawai, A. S. Foster, F. F. Canova, H. Onodera, S. Kitamura, and E. Meyer, Nat. Commun. **5**, 4403 (2014).
[9] N. Oyabu, O. Custance, I. Yi, Y. Sugawara, and S. Morita, Phys. Rev. Lett. **90**, 176102 (2003).
[10] N. Oyabu, Y. Sugimoto, M. Abe, O. Custance, and S. Morita, Nanotechnology **16**, S112 (2005).
[11] Y. Sugimoto, M. Abe, S. Hirayama, N. Oyabu, O. Custance, and S. Morita, Nat. Mater. **4**, 156 (2005).
[12] Y. Sugimoto, P. Jelinek, P. Pou, M. Abe, S. Morita, R. Perez, and O. Custance, Phys. Rev. Lett. **98**, 106104 (2007).
[13] Y. Sugimoto, P. Pou, O. Custance, P. Jelinek, M. Abe, R. Pérez, and S. Morita, Science **322**, 413 (2008).
[14] Y. Sugimoto, A. Yurtsever, N. Hirayama, M. Abe, and S. Morita, Nat. Commun. **5**, 4360 (2014).
[15] J. P. Lewis, P. Jelínek, J. Ortega, A. A. Demkov, D. G. Trabada, B. Haycock, H. Wang, G. Adams, J. K. Tomfohr, E. Abad, H. Wang, and D. A. Drabold, Phys. Status Solidi B **248**, 1989 (2011).
[16] B. Enkhtaivan and A. Oshiyama, Phys. Rev. B **94**, 085416 (2016).
[17] P. Dieška and I. Štich, Nanotechnology **18**, 084016 (2007).
[18] P. Dieška and I. Štich, Phys. Rev. B **79**, 125431 (2009).
[19] B. Enkhtaivan and A. Oshiyama, Phys. Rev. B **95**, 035309 (2017).
[20] Y. Sugimoto, K. Miki, M. Abe, and S. Morita, Phys. Rev. B **78**, 205305 (2008).
[21] Y. Sugimoto, A. Yurtsever, M. Abe, S. Morita, M. Ondráček, P. Pout, R. Pérez, and P. Jelinek, ACS Nano **7**, 7370 (2013).
[22] K. Takayanagi, Y. Tanishiro, S. Takahashi, and M. Takahashi, Surf. Sci. **164**, 367 (1985).
[23] P. Hohenberg and W. Kohn, Phys. Rev. **136**, B864 (1964).
[24] W. Kohn and L. J. Sham, Phys. Rev. **140**, A1133 (1965).
[25] J. P. Perdew, K. Burke, and M. Ernzerhof, Phys. Rev. L **77**, 3865 (1996).
[26] J. P. Perdew, K. Burke, and M. Ernzerhof, Phys. Rev. L **78**, 1396 (1997).
[27] G. Kresse and J. Hafner, Phys. Rev. B **47**, 558 (1993).
[28] G. Kresse and J. Furthmüller, Phys. Rev. B **54**, 11169 (1996).
[29] P. E. Blöchl, Phys. Rev. B **50**, 17953 (1994).
[30] G. Kresse and D. Joubert, Phys. Rev. B **59**, 1758 (1999).
[31] To check the effect of the force criteria on the calculated diffusion barriers, we calculate the barriers of the Co $\rightarrow$ H_3^L and the Ce $\rightarrow$ H_3^R diffusions of the Si adatom without the tip using the 0.01-eV/Å force convergence criterion. We find that the diffusion barriers are about 30 meV larger than those calculated with the 0.1-eV/Å force convergence criterion. Considering the energy scale of the diffusion barriers, i.e., several hundred meV, the loose criterion suffices for the present purpose.
[32] G. Henkelman, B. P. Uberuaga, and H. Jónsson, J. Chem. Phys. **113**, 9901 (2000).
[33] S. Jeong and A. Oshiyama, Phys. Rev. Lett. **81**, 5366 (1998).
[34] R. Pérez, M. C. Payne, I. Štich, and K. Terakura, Phys. Rev. Lett. **78**, 678 (1997).
[35] R. Pérez, I. Štich, M. C. Payne, and K. Terakura, Phys. Rev. B **58**, 10835 (1998).
[36] P. Dieška, I. Štich, and R. Pérez, Phys. Rev. Lett. **91**, 216401 (2003).
[37] P. Pou, S. A. Ghasemi, P. Jelinek, T. Lenosky, S. Geodecker, and R. Perez, Nanotechnology **20**, 264015 (2009).
[38] S. Jarvis, A. Sweetman, J. Bamidele, L. Kantorovich, and P. Moriarty, Phys. Rev. B **85**, 235305 (2012).
[39] H. Uchida, D. Huang, F. Grey, and M. Aono, Phys. Rev. L **70**, 2040 (1993).
[40] Here, we assume that the interaction between the tip and the surface is small when the tip-surface distance is more than 6.0/Å in Ref. [12].